

## Piece Length Types on Fish Target Strength Model

Sunardi<sup>1)</sup>, Anton Yudhana<sup>1)</sup>, Jafri Din<sup>2)</sup>

<sup>1)</sup>Electrical Engineering Department, Universitas Ahmad Dahlan(UAD)  
Kampus III Jl. Prof. Soepomo, Janturan, Umbulharjo, Yogyakarta 55164, Indonesia

<sup>2)</sup>Electrical Engineering Faculty, Universiti Teknologi Malaysia (UTM)  
Skudai, 81310 Johor Bahru, Malaysia.

### Abstract

Fish species can be identify using target strength (TS) model. The result of model compared with result from *in situ* measurement as benchmark. Selarboops (*Oxeyesca*) as commercial fish from South China Sea has been used. Lateral and dorsal X-ray of fish has been deployed to perform fish body and swim bladder morphology and then divided into a number of pieces for Kirchhoff-Ray Mode (KRM) model implementation. This model uses the various length types depend on length of pieces of swim bladder and fish body. The model has been successfully developed to identify the TS value for specific fish species. The results have been verified with results from *in situ* measurement. TS value from model is relatively similar with TS from *in situ* measurement which the difference is about 7 dB on types of r, s, and t. The result shows that type of t is better than others.

**Keywords:** Swim bladder, Target Strength, X-ray, KRM model.

### 1. INTRODUCTION

Target Strength (TS) of fish can be identified by *in situ* measurement in the natural habitats of sea or ocean and *ex situ* measurement in the laboratory experiments. *In situ* measurement incorporates ping-to-ping variability from ensonified organisms but do not permit independent measurement or the manipulation of sources that influence TS. *Ex situ* measurement using restrained fish of known length allows TS to be measured while controlling tilt and depth. TS can also be calculated by using the model approach. Theoretical calculation of TS is possible using the exact shape of the swim bladder [1]. Length, tilt, and depth influence the shape or orientation of the swim bladder also influence the amount of sound reflected by a fish [2].

Aquatic organisms are complicated scatters by nature of their shape (cylindrical or spheroid), deformation (curvature of the body and swim bladder), and composition (exoskeleton, muscle, bone, fat, presence and shape of swim bladder) [3],[4]. Fish TS is also influenced by several factors including orientation of fish relative to the transducer, the ratio of acoustic wavelength to fish length, and physiological condition

[5]. Biological variation in backscatter of fish is dependent on behavioral, morphological, ontogenetic, and physiological factors [6],[7]. Behavior includes the tilt and roll of individual organisms as well as the aggregation (i.e. shoaling) and polarized movement (i.e. schooling) by fish groups [5].

The swim bladder is considered to be responsible for most of the fish's acoustic backscattering energy [8] and consequently its TS. Natural variations in swim bladder

volume and shape may cause variation in fish TS. The important factors that are assumed to alter the TS significantly are stomach content, gonads, body-fat content, pressure, and tilt angle [9].

The swim bladder is an oval-shaped sac found in the fish's abdominal cavity, which at different times can be filled with varying amounts and compositions of gases (same as atmospheric gases; carbon dioxide, oxygen, and nitrogen). The bladder has developed as an extension of the gut wall [10]. An air-filled swim bladder can contribute up to 90% of backscattered sound [8],[11],[12]. Acoustic scattering by a swim bladder is four or more times greater than the scattering by fish bodies at any given frequency [3].

Preliminary study of target strength using commercial fish from South China Sea has been conducted through *in situ* and *ex situ* measurement [8]. We have conducted a series of *in situ* studies of commercially fish from South China Sea as in [13]-[17].

Now, in this research focus on modeling of fish target strength. X-ray images of fish body and its swim bladder has been conducted used in the development of fish acoustic model using Kirchhoff-ray mode (KRM). Review of KRM is found both in fish body and fish swim bladder [18] which modeled fish body as a set of fluid and swim bladder as gas filled cylinders [19]. KRM has been reported for several years, recently emphasis has been given on the swim bladder depth dependence [20], swimming direction [21], and validated for length and tilt [4].

KRM backscatter models have been used to characterize frequency- and behavior-dependent backscatter of

individual and aggregations of fish [18],[22]. Species-specific characteristics and metrics that facilitate the discrimination of species using acoustic [23] and illustrate the sensitivity of species-specific backscatter to assumptions of tilt-angle and material properties (densities and sound contrasts) had been identified [24]. Echo sounder properties with fish anatomy, backscatter model predictions, and fish trajectories to visualize factors that influence patterns in backscatter data can be integrated [25].

Digitized images of the fish swim bladder and body has been used with KRM model to estimate the backscatter employing a low mode cylinder solution and a Kirchhoff-ray approximation. The morphology of the fish swim bladder and fish body obtained by dissection or X-rays is used to construct finite cylinders. The coordinates has been transformed from x-z Cartesian coordinates to u-v coordinates relative to the incident wave front. Backscattering cross-sections from each finite cylinder are summed over the whole swim bladder or body and then added coherently.

TS for swim bladder and fish body are given in (1) and (2), respectively [8].

$$\ell(f) = -i \frac{R_{fs} (1 - R_{wf}^2)}{2\sqrt{\pi}} \sum_{j=0}^{N-1} A_{sb} [k_{fb} a(j) + 1]^{1/2} [e^{-i(2k_{fs} V_{fj}(j) + \psi_{sb})}] \Delta u(j) \quad (1)$$

$$\ell(f) = -i \frac{R_{wf}}{2\sqrt{\pi}} \sum_{j=0}^{N-1} [k a(j)]^{1/2} [e^{-i2k V_{fj}(j)} - (1 - R_{wf}^2) e^{-i(2k V_{fj}(j) + 2k_{fs} (V_{fj}(j) - V_{fj}(j) + \psi_{sb}))}] \Delta u(j) \quad (2)$$

Backscattering cross-section  $\sigma_{bs}$  is computed from the complex scattering length  $\ell(f)$  expressed in (3). Therefore, reduced scattering length is calculated by using (4). Equation (5) and (6) are reduced backscattering cross-section and reduced target strength, respectively. The scattering lengths for the fish body and swim bladder were computed individually. Finally, whole fish scatter can be summed from fish body and swim bladder (7).

$$\sigma_{bs}(f) = |\ell(f)|^2 \quad (3)$$

$$SL = \frac{|\ell(f)|}{TL} \quad (4)$$

$$\sigma_{bs} = \frac{|\ell(f)|^2}{TL^2} \quad (5)$$

$$TS = 20 \log_{10} \left[ \frac{\ell(f)}{TL} \right] \quad (6)$$

$$\ell_{wf}(f) = \ell_{fb}(f) + \ell_{sb}(f) \quad (7)$$

The KRM model has been applied to compute TS for Selarboops as commercially fish from South China Sea. Fish body and swim bladder are considered in the model

to develop accurate and valid results. Emphasis has been given in the implementations of various types of pieces on fish body and swim bladder. The TS results then validated using TS data from *in situ* measurement which have been deployed before.

Selarboops was deployed for *in situ* measurement and detected at 6.98 to 7.69 meters of depth. Total of 30 pings recorded with mean of TS is -46.49 dB. The model is expected to successfully provide the correct identification of TS value in accordance with the *in situ* measurement. This success will give the stolen identification of significant impact on the TS of each fish species. TS of each fish will be advised to identify using the model approach than *in situ* measurement which very expensive and difficult.

## 2. MATERIALS AND METHOD

Adult fish of 13 cm length Selarboops is used in this model. Process of X-ray to determine the morphology of fish and its swim bladder has been deployed at Health Centre of Universiti Teknologi Malaysia (UTM). The gas-filled swim bladder has a dark image because air absorbs the X-rays less than flesh. Fish morphology, position and size of swim bladder as lateral X-ray image is shown in Figure 1.

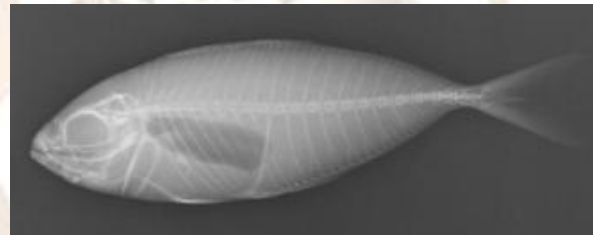


**Figure 1.** X-ray images of Selarboops

The model backscatter is representing the fish body as a contiguous set of fluid-filled cylinders that surround a set of gas-filled cylinders representing the swim bladder as shown in Figure 2.

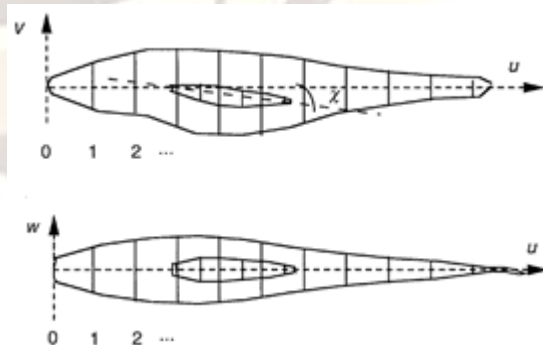


**Figure 2.** Set of fluid-filled and gas-filled cylinders [19]

Fish body and swim bladder divided into any length pieces. The number and length of pieces ( $\Delta u$ )

proportionate relatives made. Piece of swim bladder is smaller than fish body to accommodate its sensitivity of shape morphology. Length of pieces can be varies from longer (simple) to smaller (detail).

Volume and weight of swim bladder and fish body are also determined. Swim bladder and fish body percentage for each characteristic have been calculated. The percentage is increase with increasing the length.

Density ( $\rho$ ) of water ( $w$ ), fish body ( $fb$ ), and swim bladder ( $sb$ ) must be calculated as [19],[25],[26]. Density of  $fb$  and  $sb$  has been determined by ratio between weights (kg) per 1 m<sup>3</sup> volume. Sound speed ( $c$ ) through the water ( $w$ ), fish body ( $fb$ ), and swim bladder ( $sb$ ) must be calculated. Sound speed in the  $fb$  is calculated by using differences based on sound speed through the  $w$  and  $fb$ . Using density and sound speed in the water combined with density of the  $fb$  and  $sb$ , therefore sound speed through the  $fb$  and  $sb$  can be calculated.

The density of  $w$ ,  $fb$ , and swim bladder are used to determinethe ratio of density for  $fb$  to  $w$  denotes  $g$  and ratio of density for  $sb$  to  $fb$  denotes  $g'$ . Ratio of sound speed for fish body to water ( $h$ ) and ratio of sound speed for swim bladder to fish body denotes  $h'$  are used data of sound speed on water, fish body, and swim bladder.

Reflection coefficient on fish body to water interface ( $R_{wf}$ ) and reflection coefficient on swim bladder to fish body interface ( $R_{fs}$ ) are also used the density and sound speed. Frequency of 38 kHz is used in this study as used for *in situ* measurement using echo sounder. Frequency and sound speed through the water, fish body, or swim bladder are used to determine the wave number ( $k$ ).

Radius of fish body  $a(j)$ , upper surface  $V_U$ , lower surface  $V_L$ , radius of swim bladder  $a_{sb}$ , and  $vu(j)$  were described from conversion of Cartesian x-y coordinate system to u-v fish centered coordinate system. These values vary depending on individual pieces. Radius of swim bladder ( $asb$ ) and fish body ( $afb$ ) has been obtained as in [21],[25].

The KRM model was developed using MATLAB program for each species and each size. KRM model will first be used to identify the TS for swim bladder and TS for fish body. Sellarboops data is used which its swim bladder and fish body characteristics as listed in Table 1. Weight and volume of fish body and swim bladder then used to calculate the density of them. Density from this calculation then combined with parameters of water density. Sound speed in the water used to calculated sound speed in the fish body and swim bladder. Detail of density and sound speed are listed in Table 2.

**Table 1:** Swim bladder and fish body characteristics.

Parameter	Value
Weight (g)	50
Length of fish body (cm)	13

Length of swim bladder (cm)	3.47
Volume of fish body (cm <sup>3</sup> )	61
Volume of swim bladder (cm <sup>3</sup> )	3.4

**Table 2:** Density and sound speed

Parameter	Value
Density of water (kg/m <sup>3</sup> )	1030
Density of fish body (kg/m <sup>3</sup> )	1194.7
Density of swim bladder (kg/m <sup>3</sup> )	1.2
Sound speed in the water (m/s)	1490
Sound speed in the fish body (m/s)	1728.2
Sound speed in the swim bladder (m/s)	2.1699

Fish body and swim bladder data for modeling have been made using Microsoft Excel and then implemented in KRM model using Matlab program. The backscattering cross section and TS of fish species, for the fish body, swim bladder, and the whole body then identified for each specific fish.

The KRM model has been developed to identify the backscattering cross section and the TS of fish specific species and size, for the fish body, swim bladder, and the whole body. Variation on length and number of piece that used has been analysis. Length, weight, volume of fish body and swim bladder are also analyzed.

### 3. RESULT AND DISCUSSION

Both of swim bladder and fish body are divided into a certain number of pieces to get the TS value of each piece. The number of pieces can be varied in accordance with the length of each piece. Type of pieces is depends on length of piece ( $Ad$ ) and then influence to total of pieces. Types of pieces to perform KRM model independently are listed in Table 3.

**Table 3:** Type of pieces

Type of pieces	Length of pieces (mm)	Total of pieces	
		Swim bladder	Fish body
p	17.33	2	7
q	8.67	4	15
r	4.33	8	30
s	2.16	16	60
t	1.08	32	120

The program also run divided into swim bladder and fish body formula, and then detailed by types of pieces, there are p, q, r, s, and t. Figure 3 until 7 are

swim bladder TS for various types of pieces for Selarboops. Type of p is very simple. Swim bladder TS is represented by two values as graphed in Figure 3 that shows the linear correlated (1<sup>st</sup> order). Type of q represents the swim bladder TS with four value that more detailed than type p.

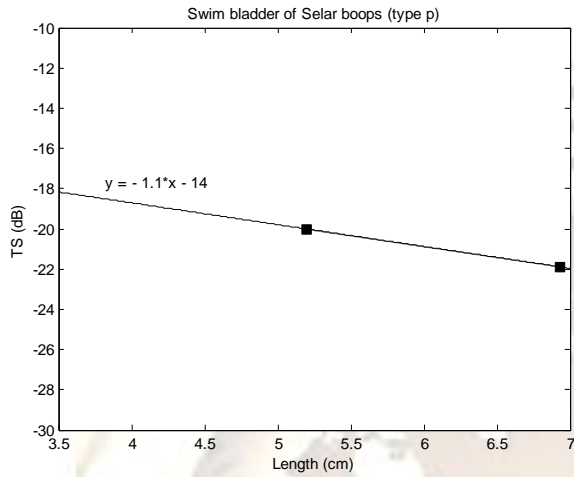


**Figure 3. Swim bladder TS (type p)**

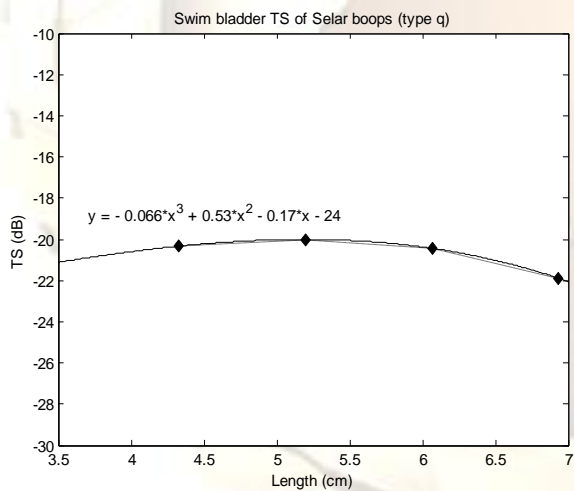


**Figure 4. Swim bladder TS (type q)**

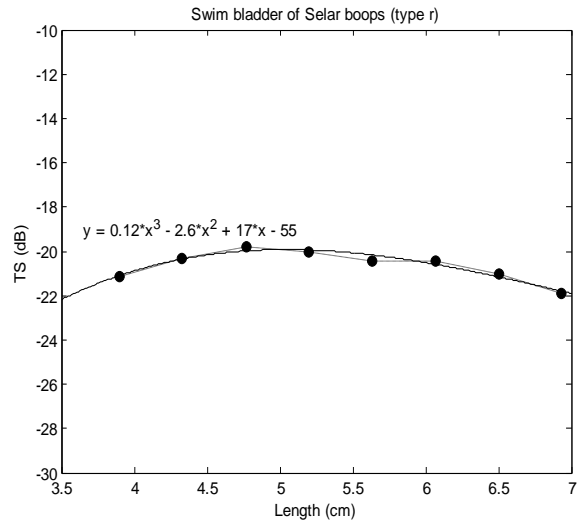


**Figure 5. Swim bladder TS (type r)**

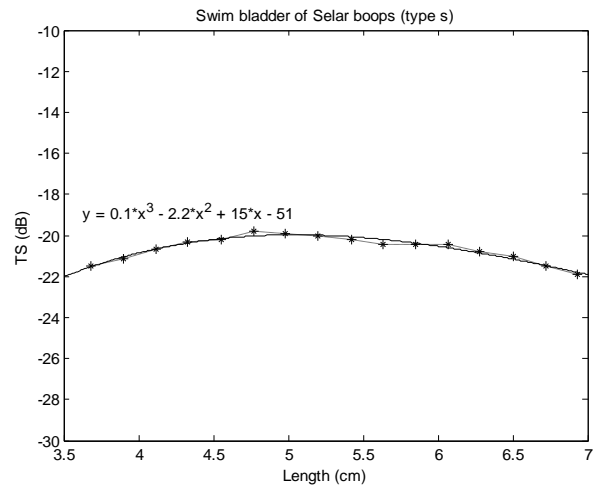


**Figure 6. Swim bladder TS (type s)**

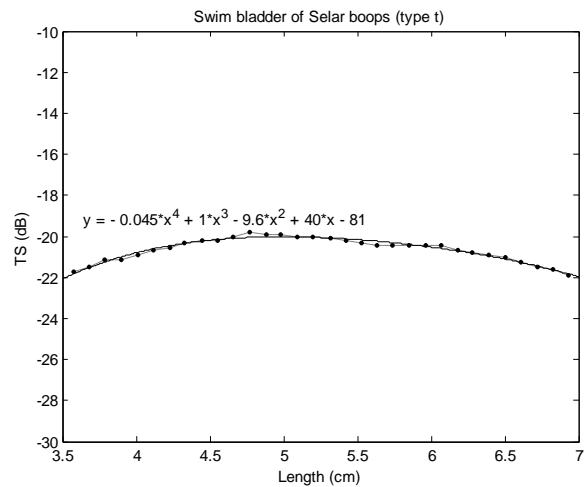


**Figure 7.** Swim bladder TS (type t)

The same way occurs in type r, s, and t that swim bladder TS shows more detailed when the number of pieces produced is increased; there are 8, 16, and 32 respectively. Type q, r, and s as graphed in Figure 4, 5, and 6 shows the quadratic correlated (2<sup>nd</sup> degree polynomial). Type t as graphed in Figure 7 shows cubic correlated (3<sup>rd</sup> degree polynomial).

TS results of swim bladder from all type of pieces can be displayed on a graph as shown in Figure 8. This graph indicates that increasing number of pieces will explain the TS results for smaller length pieces and more in detail for each piece with increasing degree of polynomial.

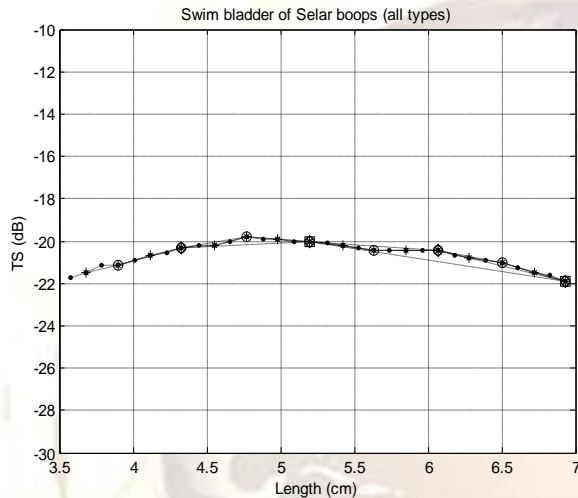


**Figure 8.** Swim bladder TS (all types)

The swim bladder TS values for each piece using type p, q, r, s, and t are listed in Table 4. Average of TS is relatively consistent on -20 dB for all types despite the different number of pieces.

**Table 4:** Swim bladder TS for each piece

The same method is used on type of p, q, r, s, and t for the fish body as shown in Figure 9 until 14. Fish body TS shows more detailed when the number of pieces is increased. Fish body TS is represented by seven values as graphed in Figure 9 that shows the cubic correlated (3<sup>rd</sup> degree polynomial). Type q and r as graphed in Figure 10 and 11 shows the 4<sup>th</sup> degree polynomial. Type s as graphed in Figure 12 shows the 5<sup>th</sup> degree polynomial. Type t as graphed in Figure 13 shows 6<sup>th</sup> degree polynomial. TS result of fish body from all type of pieces is displayed on a graph as shown in Figure 14. This graph indicates that increasing number of pieces will explain the TS results for smaller length pieces and more in detail with increasing the degree of polynomial. The fish body TS for each piece using type of p, q, r, s, and t also can be calculated as in the swim bladder. Average of each type of piece in dB is -16.854, -48.931, -48.878, -48.877, and -48.881 for type of p, q, r, s, and t

respectively. Average of fish body TS is relatively

Piec e no.	TS of various type of pieces (dB)				
	p	q	r	s	t
1.	-20.00	20.33	21.13	21.50	-21.75
2.	21.88	20.00	20.33	21.13	-21.50
3.		20.44	19.79	20.66	-21.13
4.		21.88	20.00	20.33	-21.13
5.			20.44	20.22	-20.89
6.			20.44	19.79	-20.66
7.			21.01	19.89	-20.55
8.			21.88	20.00	-20.33
9.				20.22	-20.22
10.				20.44	-20.22
11.				20.44	-20.00
12.				20.44	-19.79
13.				20.78	-19.89
14.				21.01	-19.89
15.				21.50	-20.00
16.				21.88	-20.00
17.					-20.11
18.					-20.22
19.					-20.33
20.					-20.44
21.					-20.44
22.					-20.44
23.					-20.44
24.					-20.44
25.					-20.66
26.					-20.78
27.					-20.89
28.					-21.01
29.					-21.25
30.					-21.50
31.					-21.62
32.					-21.88
Ave rage	-20.92	20.65	20.62	20.63	-20.63

consistent on -48 dB for all types despite of the different number of pieces, except for type of p.

**Figure 11.** Fish body TS (type r)

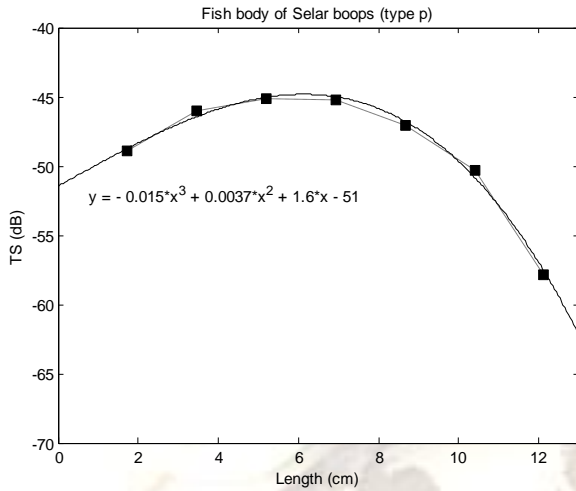


**Figure 9.** Fish body TS (type p)

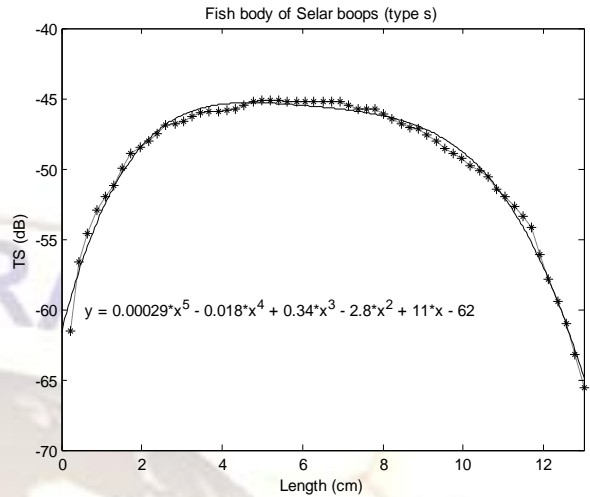


**Figure 12.** Fish body TS (type s)

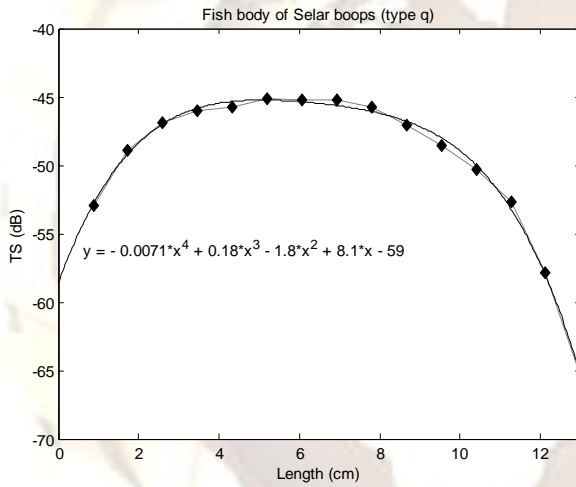


**Figure 10.** Fish body TS (type q)

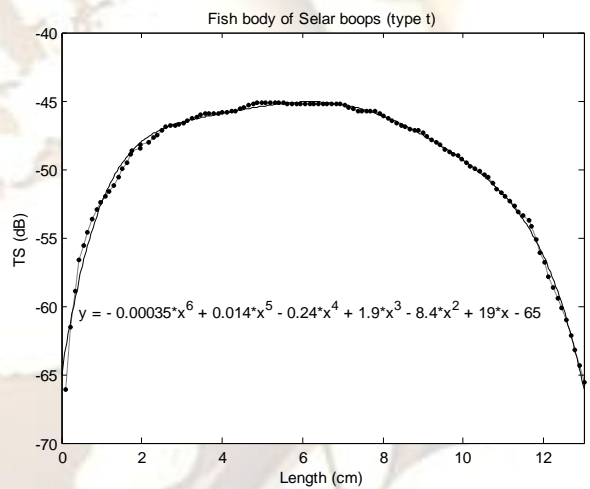


**Figure 13.** Fish body TS (type t)

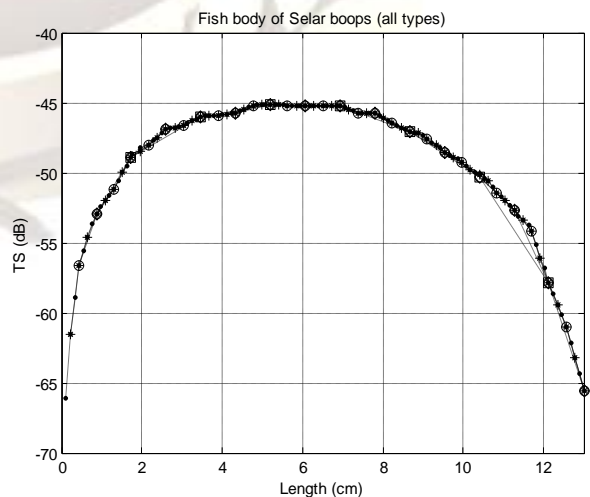
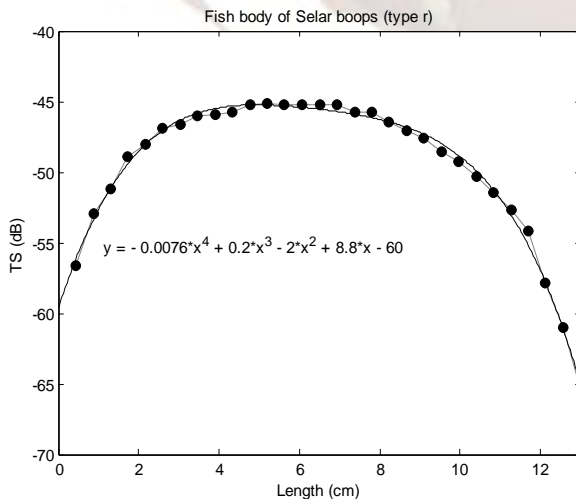


**Figure 14.** Fish body TS (all types)

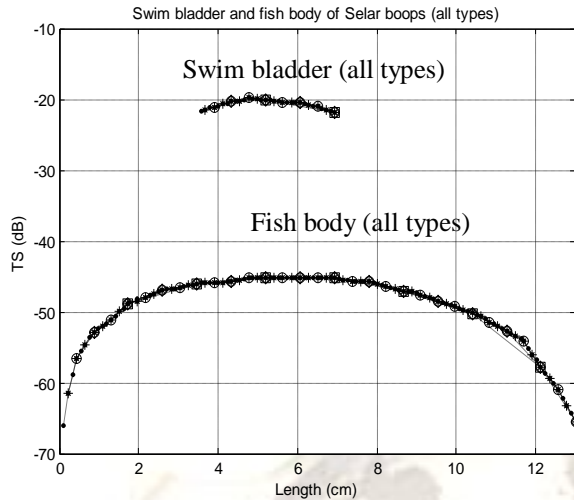


**Figure 15.** Swim bladder and fish body TS (all types)

Figure 15 is combination graph of TS for swim bladder (upper) and fish body (lower) using of all types. TS of swim bladder ( $TS_{sb}$ ) is higher than TS of fish body ( $TS_{fb}$ ) for all types. Therefore, TS is most influenced by  $TS_{sb}$  than  $TS_{fb}$ . TS of swim bladders at -20 dB are higher than fish body at -45 dB of maximum. The TS difference is more than 25 dB. This shows that swim bladder plays important to produce the TS than fish body.

TS of whole body of fish is taken from sum of TS from swim bladder and fish body. Total Length (TL) parameter is also considered in the summation. The results of the whole body TS in dB are -22.038, -37.768, -40.299, -41.392, and -41.849 for type of p, q, r, s, and t respectively. Type of r, s, and t produced whole TS relatively consistent than type of p and q.

Selarboops was deployed *within situ* measurement and detected which TS is -46.49 dB. Thus, the TS of Selarboops was successfully identified by KRM model TS differences of results from *in situ* and model is not more than 7 dB.

Much number of pieces gives consistent the TS values and used as the model results. Thus, type of scan be used for the next calculation caused by more simple and quickly running in the MATLAB software than type t but produces the relatively same results. Type of s results is enough to explain and represents the swim bladder and fish body characteristics on producing the TS as in Figure 5 and 11.

#### 4. CONCLUSION

The model has been successfully developed to identify the TS value for specific species of fish. The acoustic fish model has been verified by *in situ* measurement. These results show that the TS differences from *in situ* and KRM is not more than 7 dB. The results also show

that swim bladder is higher produce TS than fish body or the swim bladder plays an important role in determining the TS compared to fish body.

The model will be deployed for as many possible variations of species and size. Presence or absence of fish, specific species, size, and depth if it could be found will more easily for the fishermen to decide what model to install the nets.

#### ACKNOWLEDGMENT

Thanks to South East Asian Fisheries Development Center - Marine Fishery Resources Development and Management Department (SEAFDEC-MFRDMD) Terengganu Malaysia for providing Senangin II Research Vessel facilities, researchers, crew, and divers for assisting *in situ* measurement. The UTM Health Centre is thanked for assisting X-rays.

#### REFERENCES

- [1]. Foote, K.G. 1985. Rather High Frequency Sound Scattering by Swim bladder Fish. Journal of the Acoustical Society of America, 78: 688-700.
- [2]. Hazen, E.L. and Horne, J.K. 2003. A Method for Evaluating the Effects of Biological Factors on Fish Target Strength. ICES Journal of Marine Science, 60: 555-562.
- [3]. Horne, J. K. and Clay, C. J. 1998. Sonar Systems and Aquatic Organisms: Matching Equipment and Model Parameters. Canadian Journal of Fisheries and Aquatic Science, 55: 1296-1306.
- [4]. Horne, J.K. 2000. Acoustic Approaches to Remote Species Identification: a Review. Fisheries Oceanography, 9(4): 356-371.
- [5]. Horne, J.K. 2003. The Influence of Ontogeny, Physiology, and Behavior on Target Strength of Walleye pollock (*Theragra chalcogramma*). ICES Journal of Marine Science, 60: 1063-1074.
- [6]. Foote, K.G. 1990a. Averaging of Fish Target-Strength Functions. Journal of the Acoustical Society of America, 67: 504-515.
- [7]. Ona, E. 1990. Physiological Factors Causing Natural Variations in Acoustic Target Strength of Fish. Journal of the Marine Biological Association of the United Kingdom, 70: 107-127.
- [8]. Foote, K.G. 1990b. Importance of the Swim bladder in Acoustic Scattering by Fish: a Comparison of Gadoid and Mackerel Target Strengths. Journal of the Acoustical Society of America, 67: 2084-2089.
- [9]. Jorgensen, R. 2003. The Effects of Swim bladder Size, Condition, and Gonads on the Acoustic Target Strength of Mature Capelin. ICES Journal of Marine Science, 60: 1056-1062.
- [10]. Martin. 2000. Anphys Courses. [www.bio.division.edu/courses/anphys/2000/marti n.html](http://www.bio.division.edu/courses/anphys/2000/marti n.html). (accessed January 30, 2008).

- [11]. Abe, K., Sadayasu, K., Sawada, K., Ishi, K., and Takao, Y. 2004. Precise Target Strength and Morphological Observation of Juvenile Walleye pollock (*Theragra chalcogramma*). *OCEANS'04*. 9-12 November 2004. Kobe, Japan: IEEE. 2004. 370-374.
- [12]. Sawada, K., Takao, Y., and Miyanoohana, Y. 2002. Introduction of the Precise Target Strength Measurement for Fisheries Acoustics. *Turkish Journal of Veterinary Animal Science*, 26: 209-214.
- [13]. Sunardi, Hassan, R.B.R., Seman, N., Mohd, A., and Din, J. 2007a. Fish Target Strength Using Sonar. *Robotic, Vision, Information, and Signal Processing (ROVISP) Conference*, Penang Malaysia, 28-30 November 2007.
- [14]. Sunardi, Hassan, R.B.R., Seman, N., Mohd, A., and Din, J. 2007b. Target Strength Measurement of Selarboops (*Oxeye scad*) Using 38 kHz and 120 kHz. *Asia Pacific Conference on Applied Electromagnetic (APACE)*, Melaka Malaysia, 4-6 December 2007.
- [15]. Sunardi, Din, J., Yudhana, A., and Hassan, R.B.R. 2008a. In situ Fish Target Strength Measurement Compared with X-Ray Images of Swim Bladder. *International Conference on Computer and Communication Engineering (ICCCE)*, Kuala Lumpur Malaysia, 13-15 May 2008.
- [16]. Sunardi, Yudhana, A., Nawi, A.S.M., Din, J., and Hassan, R.B.R. 2008b. Target Strength Measurement of Selarboops (*Oxeye scad*) and Megalaspiscordyla (*Torpedo scad*) in South China Sea. *International Conference on Science and Technology: Applications in Industry and Education (ICSTIE)*, Penang, Malaysia, 12-13 December 2008.
- [17]. Sunardi, Din, J., Yudhana, A., and Hassan, R.B.R. 2009. Target Strength for Fish Identification Using Echo Sounder. *Journal of Applied Physics Research*, 1(2): 92-101.
- [18]. Horne, J.K. and Jech, J.M. 1999. Multi-Frequency Estimates of Fish Abundance: Constraints of Rather High Frequencies. *ICES Journal of Marine Science*, 56: 184-199.
- [19]. Clay, C.S. and Horne, J.K. 1994. Acoustic Models of Fish: The Atlantic cod (*Gadus morhua*). *Journal of the Acoustical Society of America*, 96(3): 1661-1668.
- [20]. Horne, J.K., Sawada, K., Abe, K., Kreisberg, R.B., Barbee, D.H., and Sadayasu, K. 2009. Swim bladders Under Pressure: Anatomical and Acoustic Responses by Walleye pollock. *ICES Journal of Marine Science*, 66: 1162-1168.
- [21]. Henderson, M.J., Horne, J.K., and Towler, R.H. 2008. The Influence of Beam Position and Swimming Direction on Fish Target Strength. *ICES Journal of Marine Science*, 65: 226-237.
- [22]. Jech, J.M. and Horne, J.K. 2001. Effects of *in situ* Target Spatial Distributions on Acoustic Density Estimates. *ICES Journal of Marine Science*, 58: 123-136.
- [23]. Gauthier, S. and Horne, J.K. 2004. Potential Acoustic Discrimination within Boreal Fish Assemblages. *ICES Journal of Marine Science*, 61: 836-845.
- [24]. Kloser, R.J. and Horne, J.K. 2003. Characterizing Uncertainty in Target Strength Measurement of a Deepwater Fish: Orange roughy (*Hoplostethus atlanticus*). *ICES Journal of Marine Science*, 60: 516-523.
- [25]. Mukai, T. and Iida, K. 1996. Depth Dependence of Target Strength of Live Kokanee Salmon in Accordance with Boyle's Law. *ICES Journal of Marine Science*, 53: 245-248.
- [26]. Jech, J.M., Schael, D.M., and Clay, C.S. 1995. Application of Three Sound Scattering Models to Threadfin shad (*Dorosompetenense*). *Journal of the Acoustical Society of America*, 98(4): 2262-2269.